Journal of Non-Crystalline Solids 357 (2011) 3088–3093

Contents lists available at ScienceDirect

Journal of Non-Crystalline Solids

journal homepage: www.elsevier.com/ locate/ jnoncrysol

Tensile properties of ZrCu-based bulk metallic glasses at ambient and cryogenic temperatures

L.S. Huo [a], H.Y. Bai [a], X.K. Xi [a], D.W. Ding [a], D.Q. Zhao [a], W.H. Wang [a,*], R.J. Huang [b], L.F. Li [b]

[a] Institute of Physics, Chinese Academy of Sciences, Beijing 100190, People's Republic of China
[b] Technical Institute of Physics and Chemistry, Chinese Academy of Sciences, Beijing 100190, People's Republic of China

ARTICLE INFO

Article history:
Received 18 March 2011
Received in revised form 26 April 2011
Available online 31 May 2011

Keywords:
Metallic glasses;
Mechanical properties;
Shear band

ABSTRACT

The tensile behaviors of a series of $(Zr_{47.5}Cu_{47.5}Al_5)_{1-x}(Zr_{80}Nb_{20})_x$ ($x=0$, 0.05, 0.10, 0.15) bulk metallic glasses were studied at ambient and cryogenic (77 K) temperatures. It is found that the tensile strength of the alloys increases as the temperature decreases from 298 K to 77 K. The maximum enhancement is 15.7%, and the toughness of these alloys does not deteriorate at low temperatures. We demonstrate that the higher energy required to raise the temperature in the shear bands from the cryogenic temperature to glass transition temperature is the origin of the tensile strength enhancement at low temperatures.

1. Introduction

Bulk metallic glasses (BMGs) possess unique properties, such as superior strength, high hardness, super elasticity, good corrosion resistance and high wear resistance [1–3]. These fantastic properties make the BMGs excellent candidate for structural and functional materials. The BMGs then have attracted extensive interest both in basic scientific research and application attempt during the past two decades. Considerable efforts have been made to improve the plasticity of the BMGs and to study the mechanical properties of BMGs at room temperature [4–10]. However, up to date, little is known about the mechanical behaviors especially for the tensile properties of the BMGs at cryogenic temperatures [11].

It is of great significance to investigate the mechanical properties of BMGs at low temperatures for extending the applications of the materials, such as in fields of space exploration and liquefied gas storage [12]. Previous investigations on the low temperature mechanical properties focused on the compressive behaviors. It was reported that both the compressive strength and the plastic strain prior to fracture of the Zr-based [12–14], CuZr-based [15], Cu-based [16], Ni-based [17], and Ti-based [18] BMGs, increase upon temperature decreasing, whereas the plasticity of Ce-based BMGs1 [9] declines at cryogenic temperatures. The studies of the tensile properties of $Zr_{41}Ti_{14}Cu_{12.5}Ni_{10}Be_{22.5}$ at room and low temperatures showed that the tensile strength of the BMG at room temperature is higher than that at cryogenic temperature [20]. While Kawashima et al. [11] obtained different conclusions in Zr–Cu–Al system, and they reported that the tensile strength and elongation of the alloy increase with decreasing testing temperature. Therefore, the tensile behaviors of BMGs at cryogenic temperature need to be further studied in details.

In this paper, the tensile properties of a series of $(Zr_{47.5}Cu_{47.5}Al_5)_{1-x}(Zr_{80}Nb_{20})_x$ (in atomic percentage, and $x=0$, 0.05, 0.10, 0.15) BMGs are investigated at ambient and cryogenic temperatures. We attempt to clarify the low temperature influence on the tensile behaviors of the BMGs.

2. Experimental

Alloy ingots with nominal compositions of $(Zr_{47.5}Cu_{47.5}Al_5)_{1-x}(Zr_{80}Nb_{20})_x$ ($x=0$, 0.05, 0.10, 0.15) were prepared by arc-melting mixtures of elemental Zr, Cu, Al and Nb with a purity of above 99.9% under a Ti-gettered argon atmosphere. To ensure the homogeneity, the alloy ingots were inverted and remelted at least four times, and subsequently suck-cast into a water-cooled copper mould to produce 1 mm thick plates with a width of 8 mm and length of 55 mm. The rods of alloy $x=0$ with a diameter of 5 mm and length of 85 mm were also fabricated using the same method. The fully glassy structures of the as-cast samples were verified by the differential scanning calorimetry (DSC; Perkin-Elmer DSC7, USA) and X-ray diffraction (XRD; MAC M03 XH, Cu K_α, Japan).

These BMG plates were machined into dog-bone geometry and the gauge dimensions of the specimens were 25 mm in length, 3 mm in width and 1 mm in thickness. The surfaces of the specimens were polished prior to the tensile testing, as shown in Fig. 1. The room temperature uniaxial tensile tests were carried out in an Instron electromechanical testing system 3384 (Norwood, MA) at an initial strain rate of $2\times10^{-4}\,s^{-1}$ at 298 K, with the strain measured directly

* Corresponding author. Fax: +86 10 82640223.
E-mail address: whw@iphy.ac.cn (W.H. Wang).

0022-3093/$ – see front matter © 2011 Elsevier B.V. All rights reserved.
doi:10.1016/j.jnoncrysol.2011.04.017

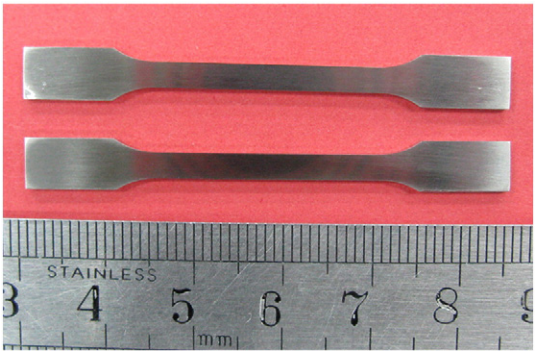

Fig. 1. The picture of the tensile specimens. The gauge dimensions are 25 mm in length, 3 mm in width, 1 mm in thickness and 8 mm in shoulder radius.

on the specimen by the extensometer. For the low temperature measurements, the specimens were immersed into the liquid nitrogen together with the tensile clamps to cool down to 77 K and the uniaxial tension was *in situ* tested in a SANS CMT 5105 (China) cryostat with an initial strain rate of $2\times10^{-4}\ s^{-1}$. Constrained by the strain-measuring devices in liquid nitrogen, the displacement of the tension clamps was precisely recorded by the testing system. Each composition was tested at least 3 times both at ambient and cryogenic temperatures. After failure, the fracture and side surfaces of the specimens were characterized by a Philips XL30 scanning electron microscope (SEM; Eindhoven, The Netherlands).

The glassy rods of $x=0$ ($Zr_{47.5}Cu_{47.5}Al_5$ BMG) were cut into short samples about 7 mm in length, with the ends polished flat and parallel to each other. The longitudinal (V_L) and transverse (V_T) acoustic velocities of the samples at different temperatures from 298 K down to 77 K were measured by the pulse-echo overlap method. The traveling time of ultrasonic waves propagating through the samples with a 10 MHz carry frequency was measured using a MATEC 6600 ultrasonic system (MATEC Inc., USA) with *x*- and *y*-cut quartz transducers. The density ρ of the samples was measured by the Archimedean technique. Then the elastic moduli (Young's modulus *E*, shear modulus *G*, and bulk modulus *K*) at different temperatures from 298 K to 77 K were derived from the V_L, V_T and ρ.

3. Results

The fully glassy structures of the as-cast samples were verified by DSC and XRD. Fig. 2(a) shows the DSC curves of the as-cast 1 mm thick plates with compositions of $(Zr_{47.5}Cu_{47.5}Al_5)_{1-x}(Zr_{80}Nb_{20})_x$ ($x=0$, 0.05, 0.10, and 0.15) with a heating rate of $20\ K\cdot min^{-1}$. The DSC traces show that the glass transition temperatures (T_g) decline as the *x* increases from 0 to 0.15 (see in Table 1). Fig. 2(b) displays the typical XRD patterns taken from the cross-section surfaces of the as-cast plates. Besides the broad diffraction maxima, no obvious peaks from crystalline phases are detected, demonstrating that all of these compositions can be fabricated into fully glassy plates with thickness of at least 1 mm by the water-cooled copper mould casting method.

3.1. Tensile properties at ambient and cryogenic temperatures

Uniaxial tension tests were conducted at ambient and cryogenic temperatures at an initial strain rate of $2\times10^{-4}\ s^{-1}$, respectively. The representative tensile engineering stress–strain curves of the $(Zr_{47.5}Cu_{47.5}Al_5)_{1-x}(Zr_{80}Nb_{20})_x$ alloys tested at room temperature are illustrated in Fig. 3(a). The specimens display initial elastic deformation behavior with an elastic strain (ε_R) of 2.0%~2.15% (as listed in Table I). Most of the BMGs fracture catastrophically without significant yielding after the elastic limits, which is usually observed in monolithic BMGs in tension tests at room temperature. The inset

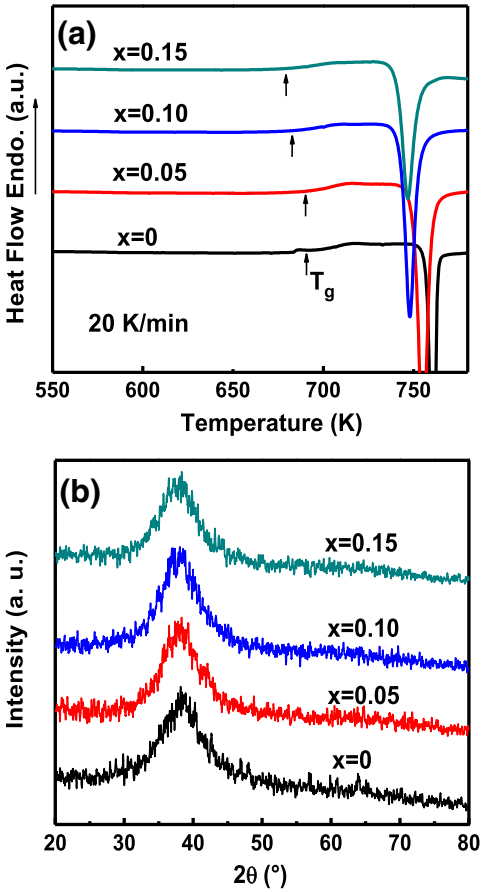

Fig. 2. (a) DSC curves and (b) XRD patterns of $(Zr_{47.5}Cu_{47.5}Al_5)_{1-x}(Zr_{80}Nb_{20})_x$ series BMG plates with thickness of 1 mm.

of Fig. 3(a) shows the magnified tensile tress-strain curve of $Zr_{47.5}Cu_{47.5}Al_5$ BMG before failure, with nearly zero observed plastic strain. However, the alloy $x=0.10$ shows a certain degree of plastic deformation sometimes, and the yield stress and plastic strain are about 1510 MPa and 0.2%, respectively. The fracture stresses of these alloys at room temperature (σ_R) are also summarized in Table 1. It can be seen that the averaged fracture stress decreases with more ZrNb addition.

Fig. 3(b) gives the typical tensile stress-displacement curves of these alloys tested at 77 K. Constrained by the strain-measuring devices at low temperatures, the displacements of the tension clamps were precisely recorded by the testing system for an approximate illustration of the elongation during tension. From the comparison of the stresses in Fig. 3(a) and (b), the fracture stress for each alloy increases dramatically when tested at 77 K, which is consistent with the results in the literature [11]. The statistical tensile fracture stresses (σ_{CT}) and the strength increments ($(\sigma_{CT}-\sigma_R)/\sigma_R$) at cryogenic temperature are summarized in Table 1. The tensile strengths for these alloys at 77 K are more than 10% higher than that at 298 K, and

Table 1
Comparison of the tensile properties of $(Zr_{47.5}Cu_{47.5}Al_5)_{1-x}(Zr_{80}Nb_{20})_x$ series BMGs tested at room and cryogenic temperatures, as well as the glass transition temperatures (T_g) and molar volumes (*V*).

Alloys	σ_R (MPa)	ε_R (%)	σ_{CT} (MPa)	$(\sigma_{CT}-\sigma_R)/\sigma_R$ (%)	T_g (K)	*V* (mm^3/mol)
$x=0$	1670±50	2.07±0.08	1910±25	14.4	691	10,380
$x=0.05$	1660±20	2.11±0.03	1920±70	15.7	690	10,489
$x=0.10$	1610±10	2.13±0.01	1840±40	14.3	683	10,663
$x=0.15$	1620±40	2.08±0.02	1810±30	11.7	679	10,853

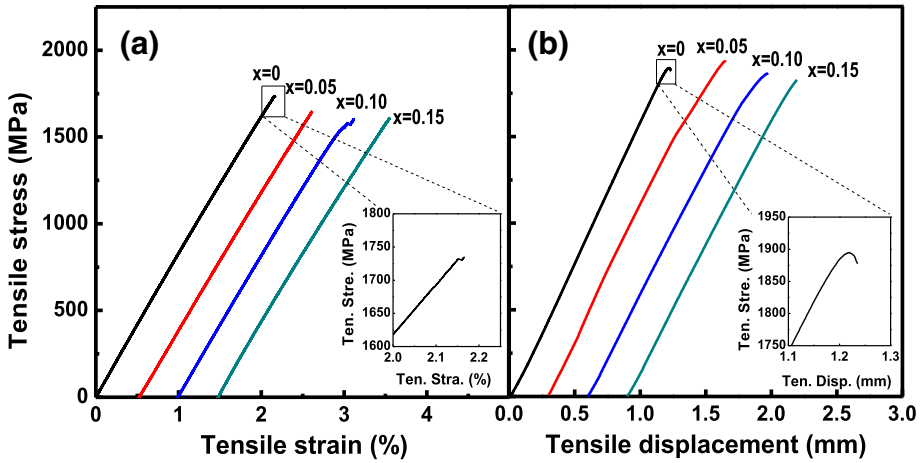

Fig. 3. (a) Tensile engineering stress–strain curves of $(Zr_{47.5}Cu_{47.5}Al_5)_{1-x}(Zr_{80}Nb_{20})_x$ series BMGs tested at 298 K, and (b) tensile stress-displacement curves of $(Zr_{47.5}Cu_{47.5}Al_5)_{1-x}(Zr_{80}Nb_{20})_x$ series BMGs tested at 77 K.

the maximum strength increment reaches about 16%. On the other hand, as shown in Fig. 3(b) and the inset, all the tensile stress-displacement curves show an obvious deviation from the initial linear stage in the end, indicating observable but small plastic deformation at 77 K before fracture. Significant tensile plasticity enhancement at the cryogenic temperature can not be obtained. This result is different from previous reports in compressive measurements at similar temperatures [11–18]. However, based on the enhancement of fracture strength and the analysis of fracture surfaces (see below), the toughness of these BMGs at least does not deteriorate with temperature decreasing down to 77 K from our results, which is markedly different from that of crystalline materials, such as steels.

3.2. The tensile fracture modes and features at room temperature and cryogenic temperature

SEM observations show that these BMGs all fracture in a shear mode both at room temperature and low temperature. Fig. 4(a) and (b) gives the representative SEM images of the side surfaces of $Zr_{47.5}Cu_{47.5}Al_5$ around the fracture location failed at room temperature and cryogenic temperature, respectively. For both cases, the formation and propagation of one major shear band dominate the failure process and the fracture occurs along a single plane. The fracture angles (θ_T) between the fracture plane and the tensile axis, clearly deviate from the angle of the maximum shear stress plane (45°) at both temperatures, and are almost equivalent, as listed in Table 2. The θ_T is in the ranges of 52°~58° and 54°~62° at room temperature and cryogenic temperature, respectively. This is consistent with the previous investigations about the tensile behaviors both at ambient and cryogenic temperatures [11,21], indicating that the role of normal stress can not be neglected in tension fracture [21,22].

Fig. 4(c) shows the side surface of the specimen of alloy $x=0.10$ early failing at ~1400 MPa tested at 77 K. It can be seen that the fracture surface is much more complex and almost perpendicular to the stress axis, similar with the case tested at ambient temperature see Fig. 3a in Ref. [22]. The unusual fracture behavior is probably caused by the heterogeneities or defects in the glassy samples, such as impurities, pores or brittle nanocrystals, in which case the fracture is mainly dominated by the defects but not the formation and propagation of the dominate shear band.

Fig. 5 shows the representative tensile fracture features of alloys $x=0$ and $x=0.15$ failed both at 298 K and 77 K. The SEM images show that the tensile fracture surfaces fractured both at room and low temperatures mainly consist of round cores with different diameters and the vein-like patterns. It is reported that the tensile fracture takes place first by the nucleation of the cores induced by the normal stress, and then by following rapid propagation of these cores towards the outside mainly driven by the shear stress, producing the combined feature of the cores and veins [21]. These cores on the fracture surfaces indicate that the normal stress still plays a significant role during the tensile fracture of BMGs even at 77 K. Small droplets are also observed on the fracture surfaces failed both at 77 K and 298 K for each composition (alloys $x=0.05$ and $x=0.10$ not shown), reflecting the decline of the viscosity within the shear bands. This indicates the temperature rise up to at least T_g in the shear bands during the tensile fracture both at 298 K and 77 K. In careful comparison of the fracture features at 298 K and 77 K, one can find that the veins patterns at 77 K are different from those at 298 K. As is shown in Fig. 5, the radiating lines from the cores (or the called veins) fractured at 77 K are straight while those at room temperature are wave-like nearly for each composition, which indicates the lower fluidity in the shear bands in the BMGs tested at 77 K. It is reasonable to deduce that the local heat within the shear bands can be more readily dissipated and the viscous flow in the shear bands becomes more difficult in the cryogenic temperature environment. And this could be the reason for the final deviation from the initial linear stage of the tensile stress-displacement curves at cryogenic temperature.

4. Discussions

Previous studies have shown that the elastic moduli of BMGs increase while decreasing the temperature [11,23], and the increase of the elastic moduli at low temperatures was considered to be main cause of the strength enhancement under cryogenic temperatures [11]. In present study, the elastic moduli of typical $Zr_{47.5}Cu_{47.5}Al_5$ BMG in the range of 77 K to 298 K were derived from the *in situ* measured V_L and V_T with decreasing the temperature from 298 K to 77 K. Fig. 6 illustrates the variations of the Young's (E), shear (G) and bulk (B) moduli with the temperature, and the E_0, G_0 and B_0 are the moduli at room temperature. It shows that the elastic moduli of the BMG monotonously increase while decreasing the temperature from 298 K to 77 K, and the variations indicate the inter-atomic bonding in the BMGs becomes stronger, which thus results the enhancement of tensile strength as the temperature decreases down to cryogenic temperature [11]. But, as shown in Fig. 6 and Table 1, the increase in Young's and shear modulus at 77 K (~5%) is far below the enhancement of tensile strength (14.4%). On the other hand, investigations pointed out that the decrease in the effective inter-atomic distance and squeeze of free volume at low temperatures,

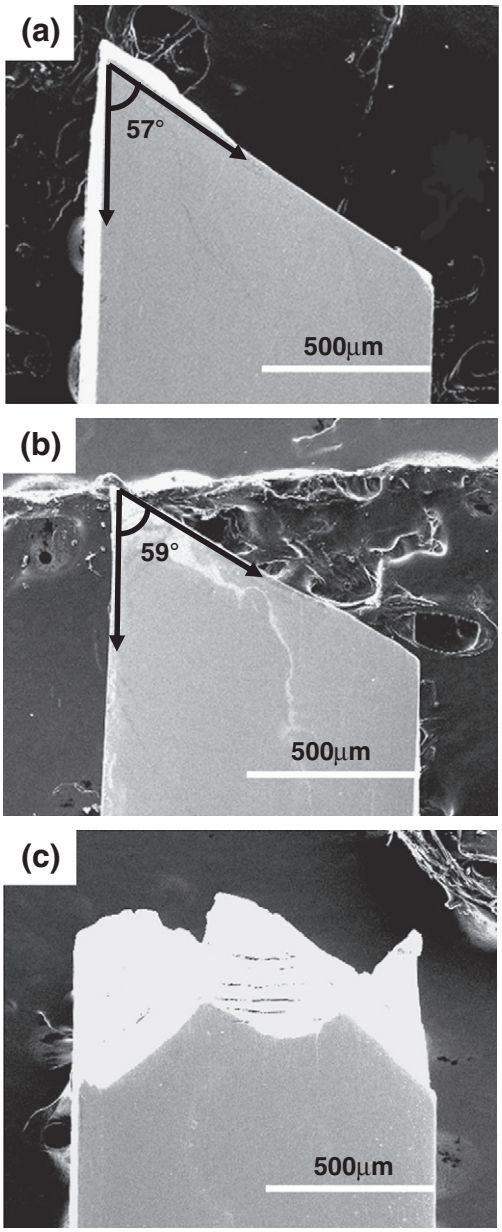

Fig. 4. SEM images of the side surfaces of tensile specimens around the fracture location. (a) $Zr_{47.5}Cu_{47.5}Al_5$ fractured at 298 K, (b) $Zr_{47.5}Cu_{47.5}Al_5$ fractured at 77 K, and (c) early fracture at ~1400 MPa of one specimen of alloy $x=0.10$ tested at 77 K.

reflected by the rising of Debye temperature Θ_D with decreasing temperature, also contribute to the strengthening [11]. Yu et al. [19] proposed that the higher energy required in the nucleation of the shear bands at cryogenic temperatures leads to the increase of yield strength. However, up to date, no quantitative relationships between the strength enhancement and the factors mentioned above have been established.

Table 2
Comparison of the tensile fracture angles (θ_T), for the $(Zr_{47.5}Cu_{47.5}Al_5)_{1-x}(Zr_{80}Nb_{20})_x$ series BMGs tested at 298 K and 77 K.

Alloys	θ_T (298 K)	θ_T (77 K)
$x=0$	55°~57°	54°~60°
$x=0.05$	54°~56°	55°~57°
$x=0.10$	52°~55°	59°~62°
$x=0.15$	53°~58°	54°~60°

Next, we attempt to quantitatively explore the origin of the tensile strength enhancement at low temperatures. In compressive deformations, the critical shear stress (τ_0) [21,22]

$$\tau_0 = \tau_y^C - \mu_C \sigma_y^C, \tag{1}$$

where τ_y^C and σ_y^C are the shear and normal yielding stresses on the shearing plane, respectively, and μ_C is a constant for the compression reflecting the effect of normal stress σ_y^C on the compressive fracture. And in tension, the critical shear stress [21,22]

$$\tau_0 = \tau_y^T + \mu_T \sigma_y^T, \tag{2}$$

where τ_y^T and σ_y^T are the shear and normal yielding stresses on the shearing plane, respectively, and μ_T is a constant for the tension reflecting the effect of normal stress σ_y^T on the tensile failure. The values of μ_C and μ_T for the BMGs have been calculated by the previous studies [21]:$\mu_C=0.07$ and $\mu_T=0.324$ for the averaged fracture angles $\theta_C=43°$ and $\theta_T=54°$ in compression and tension, respectively. Therefore, the effect of normal stress on the shearing fracture can be ignored in compression, and the critical shear stress $\tau_0 \approx \tau_y^C \approx 0.5\sigma_y^C$; whereas in tension, normal stress plays a more remarkable role in the fracture, as discussed in Section 3, and the critical shear stress should be expressed by Eq. (2).

Recently, it is found that there exist similarities between the physical processes of plastic deformation and glass transition of metallic glasses [24–27]. The tensile fracture features of the BMGs shown in Fig. 5 further confirm that the temperature in the shear bands can rise up to at least T_g both at ambient and cryogenic temperatures. Yang et al. [24] and Liu et al. [25] have proposed similar predicting equations for the strength of BMGs from the perspective of this similarity. According to the proposed universal predicting approaches for the strength of BMGs [24,25], the critical shear stress

$$\tau_0 \approx \frac{1}{V\gamma_0}\int_T^{T_g} C_p \bullet dT, \tag{3}$$

where V is the molar volume, γ_0 is the critical shear strain leading to the destabilization of the local shearing events, T is the testing temperature and C_p is the molar heat capacity at constant pressure. For solid matter, if we assume $C_p \approx C_v$, then we obtain

$$\tau_0 \approx \frac{1}{V\gamma_0}\int_T^{T_g} C_v \bullet dT, \tag{4}$$

where C_v is the molar heat capacity at constant volume.

The Debye temperature Θ_D for ZrCu-based metallic glasses is ~280 K [23,28], and therefore, when $T \geq T_R >> \Theta_D$, (T_R is room temperature) $C_v \approx 3R = 24.94\ J\cdot mol^{-1}\cdot K^{-1}$ ($R=8.314\ J\cdot mol^{-1}\cdot K^{-1}$, the molar gas constant). Then the critical shear stress at room temperature (T_R) can be expressed as follows:

$$\tau_0^{RT} = \frac{C_v\left(T_g - T_R\right)}{V\gamma_0} = \frac{3R\left(T_g - T_R\right)}{V\gamma_0}, \tag{5}$$

and the critical shear stress at cryogenic temperature is

$$\begin{aligned}\tau_0^{CT} &= \frac{1}{V\gamma_0}\left[3R\left(T_g - T_R\right) + \int_T^{T_R} 9R\left(\frac{T}{\Theta_D}\right)^3 \int_0^{\Theta_D/T} \frac{x^4 e^x}{\left(e^x-1\right)^2} dx dT\right] \\ &= \frac{1}{V\gamma_0}\left[3R\left(T_g - T_R\right) + B\right],\end{aligned} \tag{6}$$

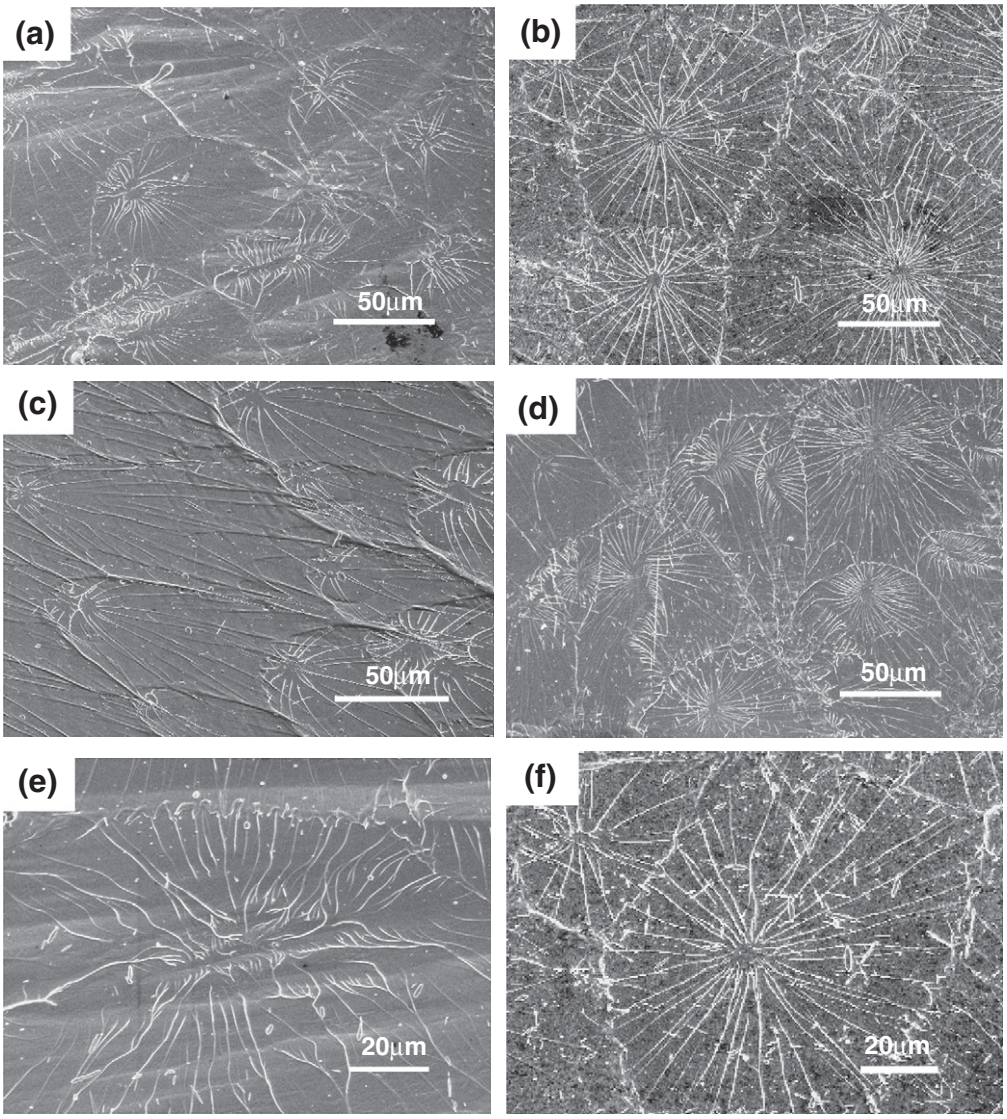

Fig. 5. Fracture features of alloys failed at 298 K and 77 K. (a) $x=0$ at 298 K, (b) $x=0$ at 77 K, (c) $x=0.15$ at 298 K, (d) $x=0.15$ at 77 K, (e) magnified pattern of alloy $x=0$ at 298 K, and (f) magnified pattern of alloy $x=0$ at 77 K.

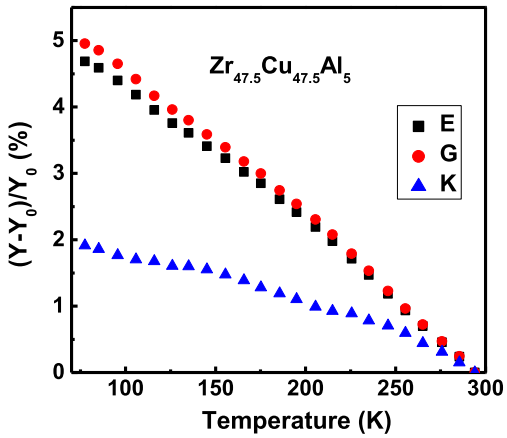

Fig. 6. The variations of E, G and B of $Zr_{47.5}Cu_{47.5}Al_5$ with the temperature.

where

$$B = \int_T^{T_R} C_v dT = \int_T^{T_R} 9R\left(\frac{T}{\Theta_D}\right)^3 \int_0^{\Theta_D/T} \frac{x^4 e^x}{(e^x-1)^2} dx dT. \quad (7)$$

In Eq. (7), the smaller T is, the larger the constant B will become. Therefore, the fact that the strength of BMGs increases as the testing temperature declines can be understood. In current work, when $T=77$ K, $B=4728$ J·mol^{-1} is calculated via Matlab and data from Ref. [29].

The value of γ_0 was estimated as $\gamma_0 \approx 1$ [30], and the critical shear stress at ambient and cryogenic temperatures can be expressed as

$$\tau_0^{RT} = \frac{3R\left(T_g - T_R\right)}{V}, \quad (8)$$

and

$$\tau_0^{CT} = \frac{3R\left(T_g - T_R\right)}{V} + \frac{B}{V}. \quad (9)$$

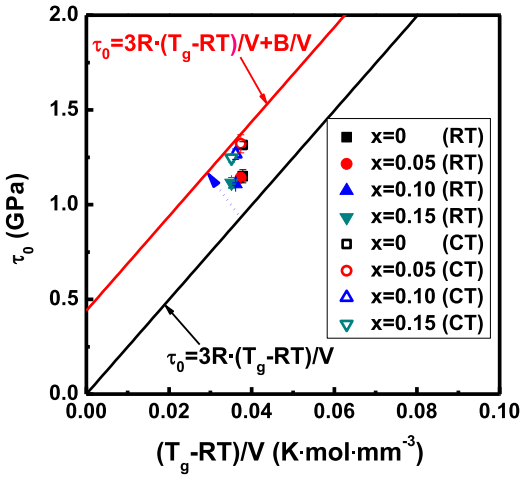

Fig. 7. The agreement between the calculated and experimental critical shear stress τ_0 at room and cryogenic temperatures.

Eq. (8) actually is the predicting unified equation for the strength of BMGs in Refs. [24] and [25]. The glass transition temperature T_g and molar volumes V of these alloys are summarized in Table 1. The difference among these molar volumes is very small, and if V is assumed to equal to the averaged value 10,600 $mm^3 \cdot mol^{-1}$ in the second term of Eq. (9), B/V is equal to ~0.45 GPa. The calculated τ_0 from Eqs. (8) and (9) versus experimental values of the 4 compositions is plotted in Fig. 7. The black line in the graph is the calculated τ_0 from Eq. (8), and the red line is for the critical shear stress at 77 K of our alloys via Eq. (9). The colored solid symbols represent the data of the alloys tested at room temperature, and the corresponding hollow ones are those tested at cryogenic temperature. The good agreement between the calculated and experimental values verifies the above equations, and provides the evidence for the origin of the strength enhancement at cryogenic temperatures. The higher energy is needed to raise the temperature in the shear bands from the cryogenic temperature to the softening temperature of the shearing medium, which is regarded at least T_g[24,25].

5. Conclusions

The tensile behaviors of $(Zr_{47.5}Cu_{47.5}Al_5)_{1-x}(Zr_{80}Nb_{20})_x$ ($x = 0$, 0.05, 0.10, 0.15) bulk metallic glasses were investigated at ambient (298 K) and cryogenic (77 K) temperatures at a strain rate of $2\times10^{-4}\ s^{-1}$.

(1) The tensile strength for these BMG alloys increase as the temperature declines from 298 K to 77 K. The enhancements of the tensile strength at 77 K for these alloys are ~14%. The tensile stress-displacement curves at 77 K show an obvious deviation from the initial linear stage in the end, implying that the toughness of these BMGs at least does not deteriorate with the temperature decreasing even to 77 K.

(2) The alloys fracture in a shear mode along a shearing plane at both temperatures, and the fracture angles between the shearing plane and stress axis are almost equivalent at 298 K and 77 K. The tensile fracture surfaces mainly consist of round cores and veins at both temperatures, but the patterns of veins at 77 K are different from those at 298 K, reflecting the larger viscosity within the shear bands at low temperature.

(3) The agreement between the experimental and calculated critical shear stresses at ambient and cryogenic temperatures demonstrates that the tensile strength enhancement at cryogenic temperatures is attributed to the higher energy needed to raise the temperature in shear bands from the cryogenic temperature to T_g.

Acknowledgements

Financial support from MOST973 of China (2010CB731603) and the NSF of China (50921091 and 50731008) is greatly appreciated. We thank M. X. Pan and Z. X. Wu for the experimental assistance and useful discussions.

References

[1] W.L. Johnson, Mater. Res. Bull. 24 (1999) 42.
[2] (a) W.H. Wang, Prog. Mater. Sci. 52 (2007) 540;
(b) W.H. Wang, Adv. Mater. 21 (2009) 4524.
[3] A.R. Yavari, J.J. Lewandowski, J. Eckert, Mater. Res. Bull. 32 (2007) 635.
[4] (a) J. Das, M.B. Tang, K.B. Kim, R. Theissmann, F. Baier, W.H. Wang, J. Eckert, Phys. Rev. Lett. 94 (2005) 205501;
(b) W.H. Wang, J.J. Lewandowski, A.L. Greer, J Mater Res. 20 (2005) 2307;
(c) M.B. Tang, D.Q. Zhao, W.H. Wang, Chin. Phys. Lett. 21 (2004) 901.
[5] Y.H. Liu, G. Wang, R.J. Wang, D.Q. Zhao, M.X. Pan, W.H. Wang, Science 315 (2007) 1385.
[6] D.C. Hofmann, J.Y. Suh, A. Wiest, G. Duan, M.L. Lind, M.D. Demetriou, W.L. Johnson, Nature 451 (2008) 1085.
[7] Y. Yokoyama, K. Fujita, A.R. Yavari, A. Inoue, Philos. Mag. Lett. 89 (2009) 322.
[8] (a) J. Pan, L. Liu, K.C. Chan, Scr. Mater. 60 (2009) 822;
(b) J.W. Qiao, S. Wang, Y. Zhang, P.K. Liaw, G.L. Chen, Appl. Phys. Lett. 94 (2009) 151905.
[9] Y. Shen, J. Xu, J. Mater. Res. 25 (2010) 375.
[10] S. Pauly, S. Gorantla, G. Wang, U. Kühn, J. Eckert, Nat. Mater. 9 (2010) 473.
[11] A. Kawashima, Y. Yokoyama, I. Seki, H. Kurishita, M. Fukuhara, H. Kimura, A. Inoue, Mater. Trans. 50 (2009) 2685.
[12] H.Q. Li, K.X. Tao, C. Fan, P.K. Liaw, H. Choo, Appl. Phys. Lett. 89 (2006) 041921.
[13] H.Q. Li, C. Fan, K.X. Tao, H. Choo, P.K. Liaw, Adv. Mater. 18 (2006) 752.
[14] Y.J. Sun, D.D. Qu, J. Shen, Y.J. Huang, X.S. Wei, Int. J. Mod. Phys. B 23 (2009) 1331.
[15] A. Kawashima, T. Okuno, H. Kurishita, W. Zhang, H. Kimura, A. Inoue, Mater. Trans. 48 (2007) 2787.
[16] K.S. Yoon, M. Lee, E. Fleury, J.C. Lee, Acta Mater. 58 (2010) 5295.
[17] A. Kawashima, Y.Q. Zeng, M. Fukuhara, H. Kurishita, N. Nishiyama, H. Miki, A. Inoue, Mater. Sci. Eng. A 498 (2008) 475.
[18] Y.J. Huang, J. Shen, J.F. Sun, Z.F. Zhang, Mater. Sci. Eng. A 498 (2008) 203.
[19] (a) P. Yu, K.C. Chan, W. Chen, L. Xia, Philos. Mag. Lett. 91 (2011) 70;
(b) J.W. Qiao, P.K. Liaw, Y. Zhang, Scr. Mater. 64 (2011) 462.
[20] X. Wang, D.C. Lou, Z.J. Gao, L. Liu, H.M. Liang, Q.F. Wang, Q. Li, M.Z. Ma, Sci. China Ser. E 48 (2005) 489.
[21] Z.F. Zhang, J. Eckert, L. Schultz, Acta Mater. 51 (2003) 1167.
[22] Z.F. Zhang, G. He, J. Eckert, L. Schultz, Phys. Rev. Lett. 91 (2003) 045505.
[23] P. Yu, R.J. Wang, D.Q. Zhao, H.Y. Bai, Appl. Phys. Lett. 90 (2007) 251904.
[24] B. Yang, C.T. Liu, T.G. Nieh, Appl. Phys. Lett. 88 (2006) 221911.
[25] Y.H. Liu, C.T. Liu, W.H. Wang, A. Inoue, T. Sakurai, M.W. Chen, Phys. Rev. Lett. 103 (2009) 065504.
[26] H.B. Yu, W.H. Wang, H.Y. Bai, Y. Wu, M.W. Chen, Phys. Rev. B 81 (2010) 220201(R.
[27] H.B. Ke, P. Wen, D.Q. Zhao, W.H. Wang, Appl. Phys. Lett. 96 (2010) 251902.
[28] W.H. Wang, J. Appl. Phys. 99 (2006) 093506.
[29] A. Tari, The Specific Heat of Matter at Low Temperatures, Imperial College Press, London, 2003.
[30] A.S. Argon, Acta Metall. 27 (1979) 47.